Multiparticle entanglement with quantum logic networks: Application to cold trapped ions

Marek Šašura[1] and Vladimír Bužek[1,2]

[1]*Institute of Physics, Slovak Academy of Sciences, Dúbravská cesta 9, Bratislava 842 28, Slovakia*
[2]*Faculty of Informatics, Masaryk University, Botanická 68a, Brno 602 00, Czech Republic*
(Received 26 December 2000; published 4 June 2001)

We show how to construct a multiqubit control gate on a quantum register of an arbitrary size N. This gate performs a single-qubit operation on a specific qubit conditioned by the state of other $N-1$ qubits. We provide an algorithm how to build up an array of networks consisting of single-qubit rotations and multiqubit control-NOT (CNOT) gates for the synthesis of an arbitrary entangled quantum state of N qubits. We illustrate the algorithm on a system of cold trapped ions. This example illuminates the efficiency of the direct implementation of the multiqubit CNOT gate compared to its decomposition into a network of two-qubit CNOT gates.

I. INTRODUCTION

Entanglement is probably the most intriguing aspect of quantum theory [1]. It attracts due attention not only for its epistemological importance [2] but also as an essential resource for quantum information processing. In particular, quantum computation [4,5], quantum teleportation [6], quantum dense coding [7], certain types of quantum key distributions [8], and quantum secret sharing protocols [9] are rooted in the existence of quantum entanglement.

Recently, a lot of progress has been achieved in the investigation of various properties and the possible application of quantum entanglement. Nevertheless, many questions are still open. In particular is the problem of multiparticle entanglement [10]. Specifically, in contrast to classical correlations, quantum entanglement cannot be freely shared among many objects [11,12]. It has been shown recently [13,14] that in a finite system of N qubits with $N(N-1)/2$ entangled pairs the maximal possible concurrence (a specific measure of entanglement [12,15]) is equal to $2/N$. This value of the bipartite concurrence is achieved when the N qubits are prepared in a totally symmetric state $|\Xi\rangle$, such that all except one qubit are in the state $|1\rangle$, i.e.,

$$|\Xi\rangle = \frac{1}{\sqrt{N}} \sum_{j=1}^{N} |0\rangle_j |1\rangle^{N-1} = \frac{1}{\sqrt{N}}(|011\ldots1\rangle + |101\ldots1\rangle$$
$$+ |110\ldots1\rangle + \cdots + |111\ldots0\rangle). \qquad (1.1)$$

In order to study the multiparticle quantum entanglement in more detail, we have to find ways how to prepare (synthesize) states of the form given by Eq. (1.1) in various physical systems.

In this paper we will study in detail how N qubits can be prepared in entangled states of the form (1.1). We assume that the qubits are encoded in internal ionic states as originally proposed in the model of the quantum processor by Cirac and Zoller [16]. Our paper is organized as follows: Section II is devoted to the description of quantum logic gates and networks. Here we present multiqubit controlled gates. We show how these gates can be expressed in terms of single-qubit and two-qubit gates, but we argue that for practical purposes it is more appropriate to utilize directly multiple-qubit gates rather than decompose them into elementary single- and two-qubit gates.

In Sec. III we present a logical network with the help of which symmetric states of the form (1.1) can be synthesized. Section IV is devoted to a general problem of synthesis of a pure state of an arbitrary N qubit state. We present a simple network in which an arbitrary N qubit state can be created. In Sec. V we apply this algorithm to a specific problem of N cold trapped ions. Following the original idea of Cirac and Zoller we show how the states of interest can be created. In Sec. VI we discuss the experimental realization of the proposed scheme on cold trapped ions and we also briefly address the efficiency of using multiqubit control-NOT gates rather than a network of two-qubit control-NOT gates.

II. QUANTUM LOGIC GATES AND NETWORKS

Let us start with a brief description of those objects that we will use later in the paper. We will follow the notation used in Refs. [3,4]. The *qubit* (quantum bit) is a quantum two-level system in which logical Boolean states 0 and 1 are represented by a pair of normalized and mutually orthogonal quantum states labeled as $|0\rangle$ and $|1\rangle$. These two states form a computational basis and any other pure state of the qubit can be written as a coherent superposition $|\psi\rangle = \alpha|0\rangle + \beta|1\rangle$ with complex amplitudes α and β, such that $|\alpha|^2 + |\beta|^2 = 1$. We may represent a state of a qubit as a point on the Bloch sphere with the parametrization $\alpha = \cos\vartheta/2$ and $\beta = e^{i\varphi}\sin\vartheta/2$. In quantum or atomic optics the qubit is often represented by a two-level atom (ion) with two selected internal levels denoted as $|g\rangle$ and $|e\rangle$. The *quantum register* of size N is a collection of N qubits. The *quantum logic gate* is a quantum device that performs a unitary operation on selected (target) qubits conditioned by states of control qubits during a given interval of time. A gate acting on a single qubit is termed as a single-qubit gate; gates acting on more qubits are referred to as multiqubit gates. The *quantum logic network* is a quantum device consisting of several quantum logic gates synchronized in time.

A. Single-qubit rotation

A single-qubit gate corresponds to a unitary operator W represented in the computational basis $\{|0\rangle, |1\rangle\}$ by the matrix
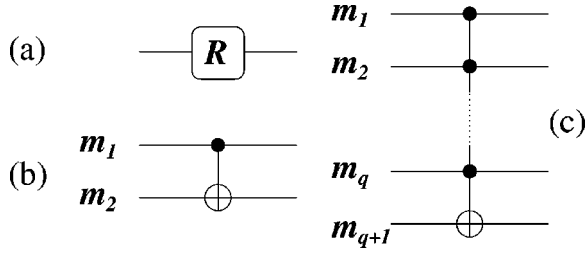
FIG. 1. A schematic representation of (a) a single-qubit rotation defined by the relation (2.2), (b) a two-qubit CNOT gate defined by the transformation (2.3), and (c) a multiqubit (control)^q-NOT gate defined by the transformation (2.4).

$$W = \begin{pmatrix} W_{00} & W_{01} \\ W_{10} & W_{11} \end{pmatrix}. \qquad (2.1)$$

A special case of a single-qubit gate is a single-qubit rotation O [see Fig. 1(a)]. Its parametrization depends on the choice of coordinates on the Bloch sphere. We will define it in the matrix form in the basis $\{|0\rangle, |1\rangle\}$ as follows:

$$O(\theta, \phi) = \begin{pmatrix} R_{00} & R_{01} \\ R_{10} & R_{11} \end{pmatrix} = \begin{pmatrix} \cos(\theta/2) & e^{i\phi}\sin(\theta/2) \\ -e^{-i\phi}\sin(\theta/2) & \cos(\theta/2) \end{pmatrix}, \qquad (2.2)$$

where θ refers to the rotation and ϕ to the relative phase shift of the states $|0\rangle$ and $|1\rangle$ in the corresponding Hilbert space.

B. Two-qubit and multiqubit control-NOT gates

A two-qubit control-NOT (CNOT) gate acts on two quantum bits denoted as the control and the target qubit, respectively [see Fig. 1(b)]. If the control qubit (m_1) is in the state $|1\rangle$, the state of the target qubit (m_2) is flipped. Otherwise, the gate acts trivially, i.e., as a unity operator $\mathbb{1}$. We may characterize this gate with the help of the truth table

$$|0\rangle_{m_1}|0\rangle_{m_2} \rightarrow |0\rangle_{m_1}|0\rangle_{m_2},$$

$$|0\rangle_{m_1}|1\rangle_{m_2} \rightarrow |0\rangle_{m_1}|1\rangle_{m_2},$$

$$|1\rangle_{m_1}|0\rangle_{m_2} \rightarrow |1\rangle_{m_1}|1\rangle_{m_2}, \qquad (2.3)$$

$$|1\rangle_{m_1}|1\rangle_{m_2} \rightarrow |1\rangle_{m_1}|0\rangle_{m_2}.$$

A multiqubit control-NOT (CNOT) gate is defined analogically [see Fig. 1(c)]. The only difference is the number of control qubits. In other words, a multiqubit (control)^q-NOT gate acts on $q+1$ qubits with q control qubits ($m_1, \ldots, m_q$) and the m_{q+1} qubit is target. If all control qubits are in the state $|1\rangle$, then the state of the target qubit is flipped. Otherwise, the gate action is trivial. The truth table of the multiqubit (control)^q-NOT gate acting on $m_1, \ldots, m_{q+1}$ qubits reads as follows:
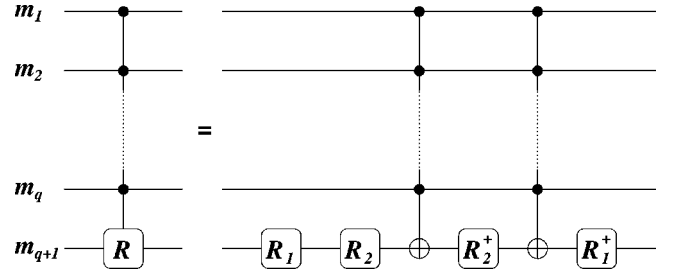
FIG. 2. A scheme of a multiqubit (control)^q-NOT gate acting on $q+1$ qubits with q control qubits ($m_1, \ldots, m_q$). The m_{q+1}th qubit is the target. The operators R, R_1, R_2, $R_2^\dagger$, and $R_1^\dagger$ are defined by Eq. (2.5) and the gate is determined by the transformation (2.6). The gate corresponding to Eq. (2.7) is represented by the same network except the single-qubit rotations R_1 and $R_1^\dagger$.

$$|\Psi_{\text{no}}\rangle|0\rangle_{m_{q+1}} \rightarrow |\Psi_{\text{no}}\rangle|0\rangle_{m_{q+1}}, \quad |\Psi_{\text{no}}\rangle \neq \prod_{j=1}^{q} \otimes |1\rangle_{m_j},$$

$$|\Psi_{\text{no}}\rangle|1\rangle_{m_{q+1}} \rightarrow |\Psi_{\text{no}}\rangle|1\rangle_{m_{q+1}},$$

$$\qquad (2.4)$$

$$|\Psi_{\text{yes}}\rangle|0\rangle_{m_{q+1}} \rightarrow |\Psi_{\text{yes}}\rangle|1\rangle_{m_{q+1}}, \quad |\Psi_{\text{yes}}\rangle = \prod_{j=1}^{q} \otimes |1\rangle_{m_j},$$

$$|\Psi_{\text{yes}}\rangle|1\rangle_{m_{q+1}} \rightarrow |\Psi_{\text{yes}}\rangle|0\rangle_{m_{q+1}}.$$

C. Multiqubit control-R gates

A multiqubit (control)^q-R gate acts on $q+1$ qubits. The $m_1, \ldots, m_q$ qubits represent the control part of the gate while the m_{q+1} qubit represents the target [Fig. 2]. This gate performs a single-qubit rotation on the target qubit if all control qubits are in the state $|1\rangle$. Otherwise, it acts trivially. Speaking precisely, if all control qubits ($m_1, \ldots, m_q$) are in the state $|1\rangle$, then the operation $R = R_1^\dagger \sigma R_2^\dagger \sigma R_2 R_1$ is applied (from right to left) on the m_{q+1} (target) qubit. In the basis of the target qubit $\{|0\rangle_{m_{q+1}}, |1\rangle_{m_{q+1}}\}$ we can introduce the matrices

$$R = \begin{pmatrix} \cos\theta & e^{i2\phi}\sin\theta \\ -e^{-i2\phi}\sin\theta & \cos\theta \end{pmatrix}, \quad \sigma = \begin{pmatrix} 0 & 1 \\ 1 & 0 \end{pmatrix},$$

$$R_1 = \begin{pmatrix} 0 & e^{i\phi} \\ -e^{-i\phi} & 0 \end{pmatrix}, \quad R_1^\dagger = \begin{pmatrix} 0 & -e^{i\phi} \\ e^{-i\phi} & 0 \end{pmatrix},$$

$$R_2 = \begin{pmatrix} \cos(\theta/2) & \sin(\theta/2) \\ -\sin(\theta/2) & \cos(\theta/2) \end{pmatrix},$$

$$R_2^\dagger = \begin{pmatrix} \cos(\theta/2) & -\sin(\theta/2) \\ \sin(\theta/2) & \cos(\theta/2) \end{pmatrix}, \qquad (2.5)$$

where $R_1 = O(\pi, \phi)$, $R_1^\dagger = O^\dagger(\pi, \phi)$, $R_2 = O(\theta, 0)$, and $R_2^\dagger = O(\theta, 0)$. The operation $O(\theta, \phi)$ is defined by the relation (2.2). The matrix σ denotes the NOT operation. If not all control qubits are in the state $|1\rangle$, then the gate performs on

the target qubit the operation $1 = R_1^\dagger 1 R_2^\dagger 1 R_2 R_1$, where 1 is the unity operator. We may write the truth table of the multiqubit $(\text{control})^q$-R gate as follows:

$$|\Psi_{no}\rangle|0\rangle_{m_{q+1}} \rightarrow |\Psi_{no}\rangle|0\rangle_{m_{q+1}},$$

$$|\Psi_{no}\rangle|1\rangle_{m_{q+1}} \rightarrow |\Psi_{no}\rangle|1\rangle_{m_{q+1}},$$

$$\text{(2.6)}$$

$$|\Psi_{yes}\rangle|0\rangle_{m_{q+1}} \rightarrow |\Psi_{yes}\rangle(\cos\theta|0\rangle_{m_{q+1}} - e^{-i2\phi}\sin\theta|1\rangle_{m_{q+1}}),$$

$$|\Psi_{yes}\rangle|1\rangle_{m_{q+1}} \rightarrow |\Psi_{yes}\rangle(e^{i2\phi}\sin\theta|0\rangle_{m_{q+1}} + \cos\theta|1\rangle_{m_{q+1}}),$$

where $|\Psi_{no}\rangle$ and $|\Psi_{yes}\rangle$ are defined in Eq. (2.4).

If the preparation of a particular class of quantum states does not require the introduction of a relative phase shift ϕ between the basis states $|0\rangle$ and $|1\rangle$, then a reduced quantum logic network is sufficient. In particular, the operation $R = \sigma R_2^\dagger \sigma R_2$ on the target qubit (m_{q+1}) conditioned by the state of control qubits $(m_1,\dots,m_q)$ can be realized according to the following truth table:

$$|\Psi_{no}\rangle|0\rangle_{m_{q+1}} \rightarrow |\Psi_{no}\rangle|0\rangle_{m_{q+1}},$$

$$|\Psi_{no}\rangle|1\rangle_{m_{q+1}} \rightarrow |\Psi_{no}\rangle|1\rangle_{m_{q+1}},$$

$$\text{(2.7)}$$

$$|\Psi_{yes}\rangle|0\rangle_{m_{q+1}} \rightarrow |\Psi_{yes}\rangle(\cos\theta|0\rangle_{m_{q+1}} - \sin\theta|1\rangle_{m_{q+1}}),$$

$$|\Psi_{yes}\rangle|1\rangle_{m_{q+1}} \rightarrow |\Psi_{yes}\rangle(\sin\theta|0\rangle_{m_{q+1}} + \cos\theta|1\rangle_{m_{q+1}}).$$

The results given above for the multiqubit control-R gates are compatible with the scheme proposed in Ref. [17], where a decomposition of multiqubit CNOT gates into a network of two-qubit CNOT gates has been presented. However, this decomposition may require many elementary operations. It seems to be more appropriate for some practical implementations of quantum computing (for example, computing with cold trapped ions [16]) to implement directly multiqubit CNOT gates.

III. QUANTUM LOGIC NETWORKS FOR THE STATE SYNTHESIS

In this section we present quantum logic networks for the synthesis of specific types of coherent superpositions of multiqubit quantum states. Later we will use this result for construction of an algorithm for a generation of an arbitrary pure quantum state of N qubits.

We will consider a quantum register of size N, i.e., N qubits. Let us denote

$$|1\rangle^N = \prod_{j=1}^{N} \otimes|1\rangle_{m_j}, \quad |1\rangle^{N-1}|0\rangle_{m_k} = \left(\prod_{\substack{j=1 \\ j \neq k}}^{N} \otimes|1\rangle_{m_j}\right) \otimes|0\rangle_{m_k}. \tag{3.1}$$

Firstly, let us consider a simple network consisting of a multiqubit control-R gate having $(N-1)$ control qubits $(c_1,\dots,c_{N-1})$ and a single target qubit (t_1) [see Fig. 3]. Let
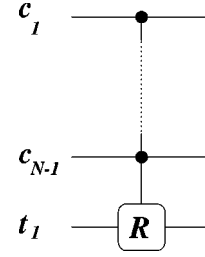
FIG. 3. The network that realizes the transformation given by Eq. (3.2).

us assume that all qubits have been initially prepared in the state $|1\rangle$, i.e., the whole system is in the state $|1\rangle^N$ and the gate realizes the operation

$$|1\rangle^N \rightarrow R_{01}|1\rangle^{N-1}|0\rangle_{t_1} + R_{11}|1\rangle^N, \tag{3.2}$$

where R_{01} and R_{11} are defined by the relation (2.5).

Secondly, let us consider a network with $(N-2)$ control qubits $(c_1,\dots,c_{N-2})$ and two target qubits (t_1,t_2) [see Fig. 4]. The network acts on the initial state $|1\rangle^N$ as follows (each arrow in the figure corresponds to an action of a gate in the sequence):

$$|1\rangle^N \rightarrow R_{01}|1\rangle^{N-1}|0\rangle_{t_1} + R_{11}|1\rangle^N$$

$$\rightarrow R_{01}|1\rangle^{N-2}|0\rangle_{t_1}|0\rangle_{t_2} + R_{11}|1\rangle^{N-1}|0\rangle_{t_2}$$

$$\rightarrow R_{01}|1\rangle^{N-2}|0\rangle_{t_1}|0\rangle_{t_2} + R_{11}|1\rangle^N. \tag{3.3}$$

Further, we design a network with $(N-3)$ control qubits $(c_1,\dots,c_{N-3})$ and three target qubits (t_1,t_2,t_3) [see Fig. 5]. This network acts as follows:

$$|1\rangle^N \rightarrow R_{01}|1\rangle^{N-1}|0\rangle_{t_1} + R_{11}|1\rangle^N$$

$$\rightarrow R_{01}|1\rangle^{N-2}|0\rangle_{t_1}|0\rangle_{t_2} + R_{11}|1\rangle^{N-1}|0\rangle_{t_2}$$

$$\rightarrow R_{01}|1\rangle^{N-3}|0\rangle_{t_1}|0\rangle_{t_2}|0\rangle_{t_3} + R_{11}|1\rangle^{N-2}|0\rangle_{t_2}|0\rangle_{t_3}$$

$$\rightarrow R_{01}|1\rangle^{N-3}|0\rangle_{t_1}|0\rangle_{t_2}|0\rangle_{t_3} + R_{11}|1\rangle^{N-1}|0\rangle_{t_3}$$

$$\rightarrow R_{01}|1\rangle^{N-3}|0\rangle_{t_1}|0\rangle_{t_2}|0\rangle_{t_3} + R_{11}|1\rangle^N. \tag{3.4}$$
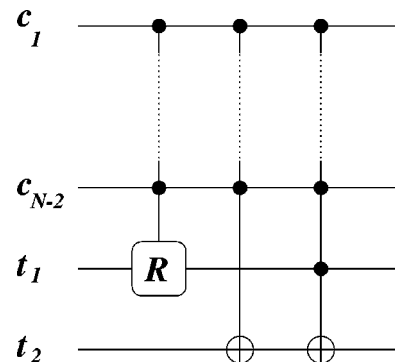
FIG. 4. The network that realizes the transformation (3.3).

FIG. 5. The network that realizes the transformation (3.4).

FIG. 7. The network for the synthesis of the generalization of the GHZ state. The single-qubit rotation R is given by Eq. (2.2) for $R = O(\pi/2, \pi)$. The initial state is $|0\rangle^N$.
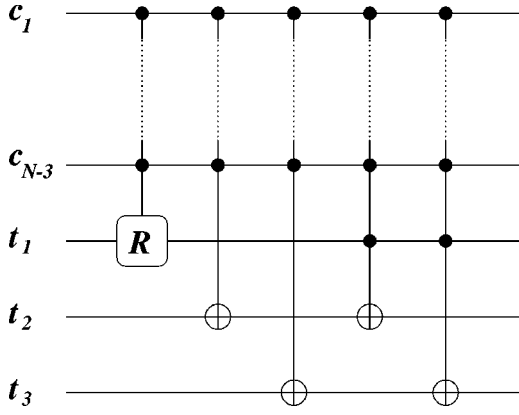
The arrangement of quantum logic networks with more target qubits is straightforward. One has to add another multiqubit CNOT gate acting on the added target qubit and then one more multiqubit CNOT gate must be included at the end of the network in order to erase ''unwanted'' changes on all other terms in a superposition state [for instance, see the fourth and fifth lines in Eq. (3.4)].

As an example let us consider a network that prepares a pure symmetric (with respect to permutations) entangled state with just one qubit in the state $|0\rangle$ and all others in the state $|1\rangle$ [see Eq. (1.1)]. It can be shown that this state exhibits the maximum degree of entanglement between any pair of N qubits [14]. The network for the synthesis of the state (1.1) from the initial state $|1\rangle^N$ is shown in Fig. 6, where the rotations U_j are defined as follows:

$$U_j = \begin{pmatrix} \sqrt{\dfrac{N-j}{N-j+1}} & \dfrac{1}{\sqrt{N-j+1}} \\ -\dfrac{1}{\sqrt{N-j+1}} & \sqrt{\dfrac{N-j}{N-j+1}} \end{pmatrix}, \quad j = 1, \ldots, N-1. \tag{3.5}$$

The action of the network in Fig. 6 can be described as follows:
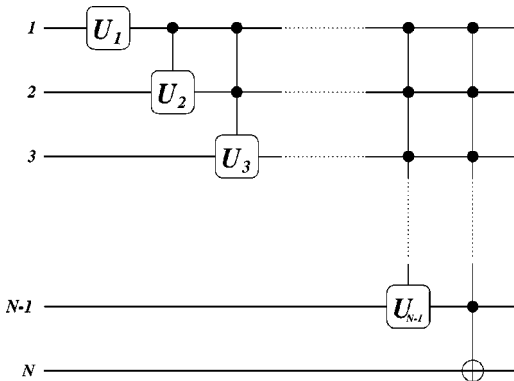
FIG. 6. The network for the synthesis of the symmetric entangled state (1.1) on N qubits. The rotations U_j are given by Eq. (3.5). The N qubits are assumed to be initially in the state $|1\rangle^N$.

$$|1\rangle^N \xrightarrow{U_1} \frac{1}{\sqrt{N}}|1\rangle^{N-1}|0\rangle_1 + \sqrt{\frac{N-1}{N}}|1\rangle^N$$

$$\xrightarrow{CU_1} \frac{1}{\sqrt{N}}|1\rangle^{N-1}|0\rangle_1 + \frac{1}{\sqrt{N}}|1\rangle^{N-1}|0\rangle_2$$

$$+ \sqrt{\frac{N-2}{N}}|1\rangle^N$$

$$\rightarrow \cdots = \frac{1}{\sqrt{N}}\sum_{j=1}^{N-2}|1\rangle^{N-1}|0\rangle_j + \sqrt{\frac{2}{N}}|1\rangle^N$$

$$\xrightarrow{CU_{N-1}} \frac{1}{\sqrt{N}}\sum_{j=1}^{N-2}|1\rangle^{N-1}|0\rangle_j + \frac{1}{\sqrt{N}}|1\rangle^{N-1}|0\rangle_{N-1}$$

$$+ \frac{1}{\sqrt{N}}|1\rangle^N$$

$$\xrightarrow{CNOT} \frac{1}{\sqrt{N}}\sum_{j=1}^{N-1}|1\rangle^{N-1}|0\rangle_j + \frac{1}{\sqrt{N}}|1\rangle^{N-1}|0\rangle_N$$

$$= \frac{1}{\sqrt{N}}\sum_{j=1}^{N}|1\rangle^{N-1}|0\rangle_j, \tag{3.6}$$

where $|1\rangle^N$ denotes the state with all qubits in the state $|1\rangle$ and $|1\rangle^{N-1}|0\rangle_j$ represents the state of the register with ($N-1$) qubits in $|1\rangle$ and the jth qubit in the state $|0\rangle$ [see the notation in Eq. (3.1)].

A very simple example is the synthesis of the GHZ state, i.e., a coherent superposition with all qubits to be in the state $|0\rangle$ or $|1\rangle$ with the same probability, i.e., $|\Xi\rangle_{\text{GHZ}} = (|0\rangle^N + |1\rangle^N)/\sqrt{2}$. The corresponding network is shown in Fig. 7. The single-qubit rotation $R = O(\pi/2, \pi)$ defined in Eq. (2.2) is applied on the initial state $|0\rangle^N$ and prepares the superposition $(|0\rangle^N + |0\rangle^{N-1}|1\rangle_1)/\sqrt{2}$. Applying sequentially all CNOT gates one prepares the GHZ state $|\Xi\rangle_{\text{GHZ}}$.
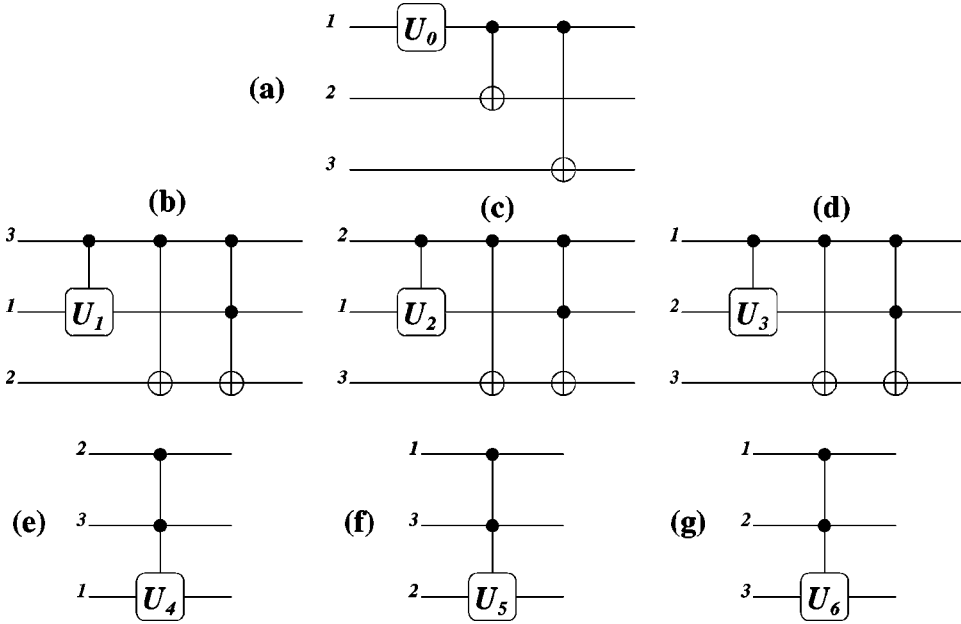
FIG. 8. An array of networks for the synthesis of an arbitrary pure quantum state (4.2) on three qubits. The initial state is $|000\rangle$ and the rotations U_j are given by Eq. (4.4).

IV. SYNTHESIS OF AN ARBITRARY PURE QUANTUM STATE

Coherent manipulation with states of quantum registers and, in particular, the synthesis of an arbitrary pure quantum state is of central importance for quantum computing. One of the important tasks is the preparation of multiqubit entangled states.

Based on the discussion presented above we can propose an array of quantum logic networks that prepare an arbitrary state from the register initially prepared in the state $|0\rangle^N$, i.e.,

$$|0\rangle^N \rightarrow |\psi(N)\rangle = \sum_{\substack{j=0 \\ x_j \in \{0,1\}^N}}^{2^N-1} c_j|x_j\rangle = \sum_{x=00...0}^{11...1} c_x|x\rangle, \quad (4.1)$$

where x is a binary representation of the number 2^j. The proposed scheme can be generalized on the quantum register of an arbitrary size, but for simplicity we will first consider the case of three qubits.

A general state of three qubits is given as

$$|\psi(3)\rangle = \alpha_0|000\rangle + e^{i\varphi_1}\alpha_1|001\rangle + e^{i\varphi_2}\alpha_2|010\rangle + e^{i\varphi_3}\alpha_3|100\rangle$$
$$+ e^{i\varphi_4}\alpha_4|011\rangle + e^{i\varphi_5}\alpha_5|101\rangle + e^{i\varphi_6}\alpha_6|110\rangle$$
$$+ e^{i\varphi_7}\alpha_7|111\rangle, \quad (4.2)$$

where $\alpha_0,\dots,\alpha_7$ are real numbers satisfying the normalization condition

$$\sum_{j=0}^{7} \alpha_j^2 = 1, \quad (4.3)$$

and $\varphi_1,\dots,\varphi_7$ are relative phase factors. The global phase is chosen such that $\varphi_0=0$.

In what follows we will present the procedure for the synthesis of the state (4.2). Let us use the abbreviated form of the matrix R defined in Eq. (2.5) which we denote as

$$U_j = \begin{pmatrix} a_j & e^{i2\phi_j}b_j \\ -e^{-i2\phi_j}b_j & a_j \end{pmatrix}, \quad j=0,\dots,6, \quad (4.4)$$

where $a_j = \cos\theta_j$ and $b_j = \sin\theta_j$. The initial state is $|000\rangle$. The network presented in Fig. 8(a) prepares out of the state $|000\rangle$ the superposition

$$a_0|000\rangle - e^{-i2\phi_0}b_0|111\rangle. \quad (4.5)$$

Applying the network in Fig. 8(b), a new term

$$-e^{i2(\phi_1-\phi_0)}b_0 b_1|001\rangle \quad (4.6)$$

is added to the superposition (4.5) while the amplitude of the component $|000\rangle$ is not affected at all. The application of the network given by Fig. 8(c) adds another new term

$$-e^{i2(\phi_2-\phi_0)}b_0 a_1 b_2|010\rangle \quad (4.7)$$

and does not influence the amplitudes of two foregoing terms $|000\rangle$ and $|001\rangle$. Repeating this procedure, the network in Fig. 8(d) adds a new term

$$-e^{i2(\phi_3-\phi_0)}b_0 a_1 a_2 b_3|100\rangle. \quad (4.8)$$

Analogously, the network shown in Fig. 8(e) adds a new term
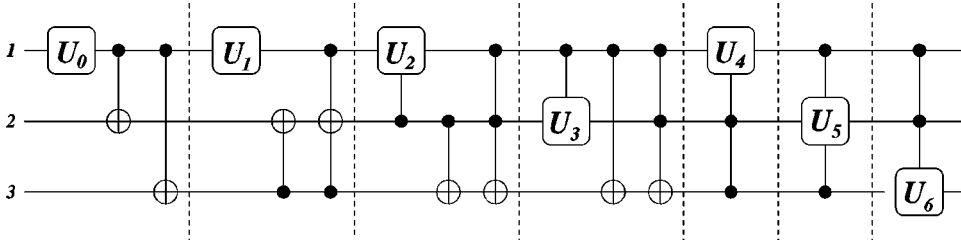
$$-e^{i2(\phi_4-\phi_0)}b_0a_1a_2a_3b_4|011\rangle, \qquad (4.9)$$

while the networks shown in Figs. 8(f) and 8(g) add new terms

$$-e^{i2(\phi_5-\phi_0)}b_0a_1a_2a_3a_4b_5|101\rangle, \qquad (4.10)$$

$$-e^{i2(\phi_6-\phi_0)}b_0a_1a_2a_3a_4a_5b_6|110\rangle, \qquad (4.11)$$

respectively. The last network shown in Fig. 8(g) also determines the amplitude of the last term

$$-e^{i2(\phi_7-\phi_0)}b_0a_1a_2a_3a_4a_5a_6|111\rangle. \qquad (4.12)$$

Comparing the output from the networks shown in Figs. 8 (see a compact form in Fig. 9), determined by the relations (4.5)–(4.12), with the expression (4.2), we get the final results in Table I..

The coherent superposition (4.2) is completely determined by 15 parameters $(\alpha_0,\ldots,\alpha_7;\varphi_1,\ldots,\varphi_7)$. The normalization condition (4.3) reduces this number to 14. The networks in Fig. 8 are determined by 14 parameters $(b_0,\ldots,b_6,\phi_0,\ldots,\phi_6)$. Thus, the mapping between the state (4.2) and the networks is clearly defined. From given values of α_j and φ_j one can calculate b_j and ϕ_j according to the expressions

$$\phi_0=\tfrac{1}{2}(\pi-\varphi_7), \quad \phi_j=\tfrac{1}{2}(\varphi_j-\varphi_7), \quad j=1,\ldots 6 \qquad (4.13)$$

and

TABLE I. The network in Fig. 9 generates the state (4.2) from an empty register $|000\rangle$. The network is characterized by the coefficients a_j,ϕ_j, where $b_j=\sqrt{1-a_j^2}$. The state (4.2) is determined by the coefficients α_j,φ_j. The table relates these two set of numbers. The inverse relations are given by Eqs. (4.13) and (4.14).

j	a_j	φ_j	State
0	a_0	0 (default)	000
1	b_0b_1	$2(\phi_1-\phi_0)+\pi$	001
2	$b_0a_1b_2$	$2(\phi_2-\phi_0)+\pi$	010
3	$b_0a_1a_2b_3$	$2(\phi_3-\phi_0)+\pi$	100
4	$b_0a_1a_2a_3b_4$	$2(\phi_4-\phi_0)+\pi$	011
5	$b_0a_1a_2a_3a_4b_5$	$2(\phi_5-\phi_0)+\pi$	101
6	$b_0a_1a_2a_3a_4a_5b_6$	$2(\phi_6-\phi_0)+\pi$	110
7	$b_0a_1a_2a_3a_4a_5a_6$	$-2\phi_0+\pi$	111

$$b_0=\sqrt{1-\alpha_0^2}, \quad b_j=\frac{\alpha_j}{\sqrt{1-\sum_{k=0}^{j-1}\alpha_k^2}}, \quad j=1,\ldots,6, \qquad (4.14)$$

which determine the single-qubit rotations (4.4).

The state (4.2) contains terms corresponding to all possible permutations of three qubits. However, a *reduced* superposition with some terms missing might be desired. For this purpose, we can skip networks responsible for the synthesis of these terms or the corresponding parameter b_j can be set to zero. For instance, in the case when the term $|000\rangle$ does not appear in a final desired quantum state, we begin with the initial state $|111\rangle$ and skip the network in Fig. 8(a). If we do not wish, for a change, to generate the term $|111\rangle$, one may set the parameter a_6 to zero and the phase factor can be chosen arbitrarily (see the table above).

The scheme can be analogically extended to an arbitrary number of qubits. In what follows we will briefly discuss the extension on four qubits. These can be prepared, in general, in the coherent superposition consisting of 16 terms, i.e., $|0000\rangle, |0100\rangle, |0010\rangle, \ldots, |1111\rangle$.

The network in Fig. 10(a) prepares the superposition of the terms $|0000\rangle$ and $|1111\rangle$ with the corresponding complex amplitudes, depending on the choice of the single-qubit rotation R_1. Application of the network in Fig. 10(b) running through all possible permutations of four qubits, i.e., $(c_1,t_1,t_2,t_3)=\{(1,2,3,4);(2,1,3,4);(3,1,2,4);(4,1,2,3)\}$, adds to the superposition new terms $|1000\rangle, |0100\rangle, |0010\rangle, |0001\rangle$ with corresponding amplitudes determined by R_2. Further, we apply the network of the type in Fig. 10(c) running through the permutations $(c_1,c_2,t_1,t_2)=\{(3,4,1,2);(2,4,1,3);(2,3,1,4);(1,4,2,3);(1,3,2,4);(1,2,3,4)\}$ and the terms $|0011\rangle,|0101\rangle,|0110\rangle,|1001\rangle,|1010\rangle, |1100\rangle$ (with corresponding amplitudes given by R_3) will be included to the state under construction. Finally, the network in Fig. 10(d) running through $(c_1,c_2,c_3,t_1)=\{(2,3,4,1);(3,4,1,2);(4,1,2,3);(1,2,3,4)\}$ generates new terms $|0111\rangle,|1011\rangle,|1101\rangle, |1110\rangle$.

The extension to N qubits is analogical. The state synthesis is started from the initial state $|0\rangle^N$. Firstly, one uses the network for the preparation of superpositions of $|0\rangle^N$ and $|1\rangle^N$ with determined amplitudes. Secondly, the networks with one control qubit (c_1) and $N-1$ target qubits $(t_1,\ldots,t_{N-1})$ running through all permutations are applied. Then, we employ the networks with two control qubits (c_1,c_2) and $N-2$ target qubits $(t_1,\ldots,t_{N-2})$. Further, the networks with more control qubits $(3,4,\ldots,N-1)$. These
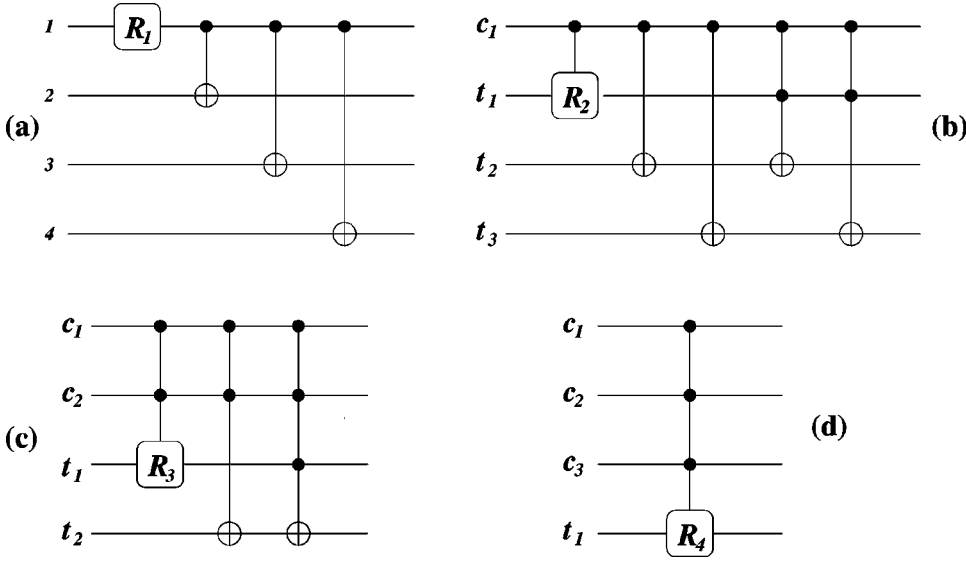
FIG. 10. An array of networks for the synthesis of an arbitrary pure quantum state (4.1) of four qubits as discussed in Sec. IV.

procedures are repeated until we achieve $N-1$ control qubits (and one target qubit). The synthesis stops and a desired final state is prepared.

V. REALIZATION ON COLD TRAPPED IONS

In previous sections we have proposed a scheme for the synthesis of an arbitrary pure quantum state of a system of N qubits. The implementation of the multiqubit CNOT gate has played the central role in our scheme. It is well known how to decompose multiqubit gates into a network of single-qubit and two-qubit CNOT gates [17]. However, it seems that a direct implementation of multiqubit CNOT gates in specific quantum systems is more straightforward and requires less elementary operations (for example, laser pulses) than its decomposition. We demonstrate this idea on a system of *cold trapped ions*. We will briefly describe the system under consideration and show how multiqubit gates can be implemented.

The quantum system considered here is a model of a string of N atomic ions confined in the linear Paul trap proposed by Cirac and Zoller in 1995 [16]. First experiments on a single ion and two ions were realized by the NIST group in Boulder [18]. Experiments with more ions were done, for example, by the group in Innsbruck [19].

The confinement of a system of trapped ions along the x, y, and z axes can be described by an anisotropic harmonic pseudopontential of frequencies $\omega_z \ll \omega_r$, where for the usual choice of trapping radio-frequency (rf) voltage we get $\omega_r = \omega_x = \omega_y$. The ions are firstly Doppler cooled and then undergo the sideband cooling. Laser cooling minimizes their motional energy and the ions oscillate around their equilibrium positions. In this case we can describe their motion in terms of normal modes. We will consider only the lowest, center-of-mass (COM), vibrational collective mode of the ions along the z axis, when all the ions oscillate back and forth as if they were a rigid body. The sideband cooling leaves the ions in the quantum ground motional state; therefore, we have to assume the Lamb-Dicke limit, i.e., the photon recoil frequency (corresponding to the laser-cooling tran-

sition) is much smaller than the frequency of the considered COM mode. The ions in the trap represent qubits with two distinct internal atomic states denoted as $|g\rangle$ and $|e\rangle$ with corresponding energy levels E_g and E_e, respectively. We will consider individual-ion-addressing with a laser beam of the frequency ω_L represented by a classical traveling wave. Then, in the interaction picture, in the rotating-wave approximation plus the weak-coupling regime and in the Lamb-Dicke limit we can write the Hamiltonian corresponding to the interaction between the jth trapped ion ($j=1,\ldots,N$) and the laser beam tuned on the *carrier* ($\omega_L=\omega_0$)

$$\hat{A}_j = \frac{\hbar \Omega_j}{2}(|e\rangle_j\langle g| + |g\rangle_j\langle e|) \tag{5.1}$$

and on the *first red sideband* ($\omega_L=\omega_0-\omega_z$)

$$\hat{B}_j = \frac{\hbar \Omega_j}{2}\frac{i\eta}{\sqrt{N}}(|e\rangle_j\langle g|\hat{a} + |g\rangle_j\langle e|\hat{a}^\dagger), \tag{5.2}$$

where $\Omega_j = |\Omega_j|e^{-i\phi}$ is the laser coupling constant, ϕ is the laser phase, η is the Lamb-Dicke parameter, $\hat{a}$ and $\hat{a}^\dagger$ are the annihilation and creation operators of the quantized COM mode with the frequency ω_z, where $\hat{a}^\dagger\hat{a}|n\rangle = n|n\rangle$ and $\omega_0 = (E_e-E_g)/\hbar$ is the atomic transition frequency.

Further, we can write the unitary evolution operators via which the action of the quantum gates is realized. Firstly, let us consider the evolution operator corresponding to a $k\pi$ pulse on the carrier ($t=k\pi/|\Omega_j|$) applied on the jth ion with the arbitrary initial choice of the laser phase such that

$$\hat{A}_j^k(\phi) = \exp\left[-\frac{k\pi}{2}(|e\rangle_j\langle g|e^{-i\phi} - |g\rangle_j\langle e|e^{i\phi})\right]. \tag{5.3}$$

Under the action of this unitary operator the two internal states of the jth ion are changed as follows:

$$|g\rangle_j \to \cos(k\pi/2)|g\rangle_j - e^{-i\phi}\sin(k\pi/2)|e\rangle_j,$$

$$|e\rangle_j \to \cos(k\pi/2)|e\rangle_j + e^{i\phi}\sin(k\pi/2)|g\rangle_j. \tag{5.4}$$

Secondly, we have the evolution operator for a $k\pi$ pulse on the first red sideband ($t = k\pi\sqrt{N}/|\Omega_j|\eta$) on the jth ion choosing the laser phase such that

$$\hat{B}_j^{k,q}(\phi) = \exp\left[-\frac{ik\pi}{2}(|e_q\rangle_j\langle g|\hat{a}e^{-i\phi} + |g\rangle_j\langle e_q|\hat{a}^\dagger e^{i\phi})\right], \tag{5.5}$$

which implies the transformation

$$|g\rangle_j|0\rangle \rightarrow |g\rangle_j|0\rangle,$$

$$|g\rangle_j|1\rangle \rightarrow \cos(k\pi/2)|g\rangle_j|1\rangle - ie^{-i\phi}\sin(k\pi/2)|e\rangle_j|0\rangle, \tag{5.6}$$

$$|e\rangle_j|0\rangle \rightarrow \cos(k\pi/2)|e\rangle_j|0\rangle - ie^{i\phi}\sin(k\pi/2)|g\rangle_j|1\rangle,$$

where $q = $ I, II, and $|e_I\rangle$ denotes the upper internal level, whereas $|e_{II}\rangle$ refers to an auxiliary internal level $|aux\rangle$. In the original proposal [16] the values of the parameter $q = $ I, II refer to the situation where the transition excited by the laser depends on the laser polarization.

The operators (5.3) and (5.5) provide us with the possibility of introducing the implementation of the single-qubit rotation and multiqubit CNOT gate on selected ions (representing qubits). It is obvious from the transformation (5.4) that the evolution operator (5.3) corresponds to the single-qubit rotation $O(k\pi, \phi)$ on the jth ion [see the definition (2.2)]. The two-qubit CNOT gate (the m_1th ion is the control and the m_2th ion is the target) is realized by the evolution operator (from right to left)

$$\hat{\mathcal{A}}_{m_2}^{1/2}(\pi)\hat{\mathcal{B}}_{m_1}^{1,\text{I}}\hat{\mathcal{B}}_{m_2}^{2,\text{II}}\hat{\mathcal{B}}_{m_1}^{1,\text{I}}\hat{\mathcal{A}}_{m_2}^{1/2}(0), \tag{5.7}$$

which corresponds to a sequence of pulses as described above. This transformation acts on two ions as

$$|g\rangle_{m_1}|g\rangle_{m_2}|0\rangle \rightarrow |g\rangle_{m_1}|g\rangle_{m_2}|0\rangle,$$

$$|g\rangle_{m_1}|e\rangle_{m_2}|0\rangle \rightarrow |g\rangle_{m_1}|e\rangle_{m_2}|0\rangle,$$

$$\tag{5.8}$$

$$|e\rangle_{m_1}|g\rangle_{m_2}|0\rangle \rightarrow |e\rangle_{m_1}|e\rangle_{m_2}|0\rangle,$$

$$|e\rangle_{m_1}|e\rangle_{m_2}|0\rangle \rightarrow |e\rangle_{m_1}|g\rangle_{m_2}|0\rangle.$$

The ions are assumed to be cooled to the ground vibrational state $|0\rangle$ before the operation. We have used the notation $\hat{B} \equiv \hat{B}(0)$ in the relation (5.7). The two-qubit CNOT gate can be extended to the multiqubit (control)^q-NOT gate acting on $q + 1$ ions ($m_1,\ldots,m_q$ ions represent the control, while the m_{q+1}th ion is the target) and can be realized by the following evolution operator (from right to left):

$$\hat{\mathcal{A}}_{m_{q+1}}^{1/2}(\pi)\hat{\mathcal{B}}_{m_1}^{1,\text{I}}\left[\prod_{j=2}^{q}\hat{\mathcal{B}}_{m_j}^{1,\text{II}}\right]\hat{\mathcal{B}}_{m_{q+1}}^{2,\text{II}}\left[\prod_{j=q}^{2}\hat{\mathcal{B}}_{m_j}^{1,\text{II}}\right]\hat{\mathcal{B}}_{m_1}^{1,\text{I}}\hat{\mathcal{A}}_{m_{q+1}}^{1/2}(0) \tag{5.9}$$

corresponding to the transformation

$$|\Psi_{\text{no}}\rangle|g\rangle_{m_{q+1}}|0\rangle \rightarrow |\Psi_{\text{no}}\rangle|g\rangle_{m_{q+1}}|0\rangle, \quad |\Psi_{\text{no}}\rangle \neq \prod_{j=1}^{q}\otimes|e\rangle_{m_j},$$

$$|\Psi_{\text{no}}\rangle|e\rangle_{m_{q+1}}|0\rangle \rightarrow |\Psi_{\text{no}}\rangle|e\rangle_{m_{q+1}}|0\rangle,$$

$$|\Psi_{\text{yes}}\rangle|g\rangle_{m_{q+1}}|0\rangle \rightarrow |\Psi_{\text{yes}}\rangle|e\rangle_{m_{q+1}}|0\rangle,$$

$$|\Psi_{\text{yes}}\rangle = \prod_{j=1}^{q}\otimes|e\rangle_{m_q},$$

$$|\Psi_{\text{yes}}\rangle|e\rangle_{m_{q+1}}|0\rangle \rightarrow |\Psi_{\text{yes}}\rangle|g\rangle_{m_{q+1}}|0\rangle. \tag{5.10}$$

It is obvious from Eqs. (5.8) and (5.10) that the ions must be kept in the ground motional state. This arrangement eliminates heating processes that lead to decoherence. However, it is still an experimental challenge to cool more than two ions to the ground state $|n = 0\rangle$.

VI. DISCUSSION AND CONCLUSIONS

In this paper we have shown how multiparticle entangled states can be constructed with the help of multiqubit quantum gates. We have shown how to implement these gates on the system of cold trapped ions. This allows us to "realize" any multiqubit control-R gate and also any logic network proposed in Secs. III and IV. To understand the feasibility of this algorithm we present some estimations considering the application of the introduced gates and networks on cold trapped ions.

The main aim of further discussion is to illustrate a range of relevant physical parameters for implementation of proposed scheme. Obviously, specific experimental setups have to be considered separately. We present just rough estimates of minimal times required for the realization of desired gate operations.

Let us consider calcium ions ^{40}Ca$^+$ with the "ground" (computational) state $|g = S_{1/2}\rangle$ and the "excited" (computational) state $|e = D_{5/2}\rangle$. The lifetime of the ion on the metastable $D_{5/2}$ level is 1.045 s.

We will assume N ions loaded and confined in the trap. The ions will be individually addressed with a laser beam ($\lambda = 729$ nm) supposing the Gaussian intensity profile $I/I_0 = \exp(-2\rho^2/w_0^2)$, where ρ denotes the radial distance and $2w_0 = 10\ \mu$m is the beam waist. Further, let the angle between the laser beam and the z axis be $\vartheta = 60°$. Then, the recoil frequency of the calcium ion is $f_R = 2.33$ kHz, where $f_R = E_R/h$, $E_R = \hbar^2k^2/2m$, $k = 2\pi/\lambda$, and $h = 2\pi\hbar$. The axial trapping frequency is $\omega_z/2\pi = 110$ kHz. We can also calculate the Lamb-Dicke parameter $\eta = \sqrt{E_R/\hbar\omega_z}$, i.e., $\eta = 0.15$. The minimum spacing between two neighboring ions is determined by the approximate formula [20,21],

$$\Delta z_{\min} \simeq \frac{2.018}{N^{0.559}}\left(\frac{q^2}{4\pi\varepsilon_0 m\omega_z^2}\right)^{1/3}, \tag{6.1}$$

where q is the ion charge, m is the ion mass, and ϵ_0 is the permitivity of vacuum.

TABLE II. N is the number of calcium ions in the trap, $\Delta z_{\min}$ is the minimal distance between two neighboring ions (6.1), $T_{\mathcal{B}}$ is the minimal time for the realization of the operation $\mathcal{B}^1$ [in Eq. (5.9)] for two different values of the fidelity ($F=99\%$, $F=75\%$). $N(\mathcal{A})$ is the total number of the operations $\mathcal{A}$ in the network in Fig. 6, and $N(\mathcal{B}^1)$ and $N(\mathcal{B}^2)$ are the total numbers of the operations $\mathcal{B}^1$ and $\mathcal{B}^2$, respectively. T is the total minimal time (6.3) for the experimental preparation of the state (1.1) on N ions via the network in Fig. 6. $T_{\mathcal{A}}=5\ \mu s$ is the time for the realization of the operation $\mathcal{A}$ [in Eq. (5.9)].

		$T_{\mathcal{B}}$ (μs)					T (ms)	
N	$\Delta z_{\min}$ (μm)	$F=99\%$	$F=75\%$	$N(\mathcal{A})$	$N(\mathcal{B}^1)$	$N(\mathcal{B}^2)$	$F=99\%$	$F=75\%$
2	24.4	312	62.4	3	2	1	1.26	0.265
3	20.8	382	76.4	9	8	3	5.39	1.11
4	18.0	441	88.3	15	18	5	12.4	2.55
5	15.9	493	98.7	21	32	7	22.8	4.65
6	14.3	540	108	27	50	9	36.9	7.48
7	13.1	584	117	33	72	11	55.1	11.2
8	12.2	624	125	39	98	13	77.6	15.7
9	11.4	662	132	45	128	15	105	21.1
10	10.8	698	140	51	162	17	137	27.7
15	8.59	855	171	81	392	27	382	76.7
20	7.31	987	197	111	722	37	786	157

The multiqubit CNOT gate on the ions is realized by the evolution operator (5.9). We will consider three types of elementary operations: (1) $\pi/2$ pulse on the carrier ($\mathcal{A}$) defined by the relation (5.3), (2) π pulse ($\mathcal{B}^1$), and (3) 2π pulse ($\mathcal{B}^2$) on the first red sideband (5.5). Each elementary operation takes a certain time to be implemented on the system of cold trapped ions. Steane *et al.* addressed in detail the speed of ion-trap information processors in [22].

First, the single-qubit rotation ($\mathcal{A}$) can be made much faster than two-qubit operations ($\mathcal{B}^1,\mathcal{B}^2$), because the Lamb-Dicke parameter η can be set to zero (i.e., the laser beam is perpendicular to the z axis). Thus, $|\Omega|$ can be made large without restrictions on the weak-coupling regime characterized by the condition $|\Omega|\ll\omega_z$. We will assume $|\Omega|/2\pi=50\ \text{kHz}$ and estimate the time required for the single-qubit rotation as $T_{\mathcal{A}}=\pi/2|\Omega|=5\ \mu s$.

Second, by definition for the operations $\mathcal{B}^1$ and $\mathcal{B}^2$, the Lamb-Dicke parameter must be nonzero [see Eq. (5.2)]. This means that some unwanted off-resonant transitions will be present, which may significantly affect times required for the operations $\mathcal{B}^{1,2}$.

In Ref. [22] it has been shown that the minimal speed $1/T_{\mathcal{B}}$ for the realization of the operation $\mathcal{B}^1$ is proportional to the geometric mean of the recoil and trapping frequency, i.e.,

$$\frac{1}{T_{\mathcal{B}}}\simeq\frac{2\sqrt{2}\epsilon}{\sqrt{N}}\sqrt{\frac{E_R}{h}\frac{\omega_z}{2\pi}}, \qquad (6.2)$$

where the imprecision $\epsilon=\sqrt{1-F}$ is defined via the fidelity F of the process. The time for the operation $\mathcal{B}^2$ is then $2T_{\mathcal{B}}$.

Once the gate times are estimated, we can determine the minimal total time T required for the experimental preparation of the state (1.1) on calcium ions. The total time T is the sum of times of all operations $\mathcal{A}$, $\mathcal{B}^1$, $\mathcal{B}^2$, which appear in the implementation of the network in Fig. 6. The total number of all operations, when preparing the state (1.1) on N ions, is $2N^2+4N-10$. The explicit expression for the total time reads

$$T=N(\mathcal{A})T_{\mathcal{A}}+N(\mathcal{B}^1)T_{\mathcal{B}}+N(\mathcal{B}^2)2T_{\mathcal{B}}. \qquad (6.3)$$

In what follows we will consider several situations with the number of trapped ions varying from 2 to 20. In a given ion trap for different values of ions we obtain different minimal spacings $\Delta z_{\min}$ [see Eq. (6.1)]. The minimal spacing between ions has to be larger than the half-width of the Gaussian profile of the addressing laser beam. In the Innsbruck experiment [23] the width of the Gaussian profile is proportional to $10\mu m$. Even for 20 ions with $\Delta z_{\min}=7.31\ \mu m$ [see Eq. (6.1)] and the given width of the Gaussian profile, the ratio between the light intensity of the laser addressing a given ion to the intensity of the same beam on the neighboring ion is as small as 1.4%. Therefore, individual ions can be addressed rather efficiently.

As follows from Eq. (6.2) the minimal time for the gate operation depends on the required fidelity of the process. In our case we consider two values of the fidelity, namely $F=99\%$ and $F=75\%$. Given these values we can estimate relevant physical parameters.

In Table II we present results of our estimations. From here we can conclude that for a given lifetime of calcium ions (1.045 s) one can perform in our scheme a coherent manipulation with up to 20 ions with the fidelity 99%. It seems to be a very optimistic estimation; however, we did not optimize the network itself.

We have chosen the cold trapped ions as an example for the situation when the direct implementation of the multiqubit CNOT gate (using elementary operations, i.e., in this case laser pulses) is much less demanding than the decomposition of multiqubit CNOT gates into the network of two-qubit CNOT gates. For instance, let us consider the multiqubit CNOT gate

on six qubits. Using the results of Ref. [17] we can decompose this multiqubit CNOT gate into the network composed of 12 two-qubit CNOT gates. In addition, this network had to be extended by three additional auxiliary qubits. The multibit CNOT gate on N ions (5.9) is realized by $2N+1$ laser pulses. Each two-qubit CNOT gate on two ions is then realized using five laser pulses (5.7). It means that all together 60 pulses have to be used for 12 two-qubit CNOT gates. However, the direct implementation of the multiqubit CNOT gate on six ions requires only 13 laser pulses. This difference becomes even more significant with the increasing number of the ions. Obviously, the smaller the number of pulses the easier the scheme can be implemented.

---

[1] E. Schrödinger, Naturwissenschaften **23**, 807 (1935); **23**, 823 (1935); **23**, 844 (1935).

[2] A. Einstein, B. Podolsky, and N. Rosen, Phys. Rev. **47**, 777 (1935); J. S. Bell, Physics (Long Island City, N.Y.) **1**, 195 (1964); A. Peres, *Quantum Theory: Concepts and Methods* (Kluwer, Dordrecht, 1993).

[3] A. Ekert, P. Hayden, and H. Inamori, e-print quant-ph/0011013.

[4] M. A. Nielsen and I. L. Chuang, *Quantum Computation and Quantum Information* (Cambridge University Press, Cambridge, 2000).

[5] J. Gruska, *Quantum Computing* (McGraw-Hill, New York, 1999).

[6] C. H. Bennett, G. Brassard, C. Crépeau, R. Jozsa, A. Peres, and W. K. Wootters, Phys. Rev. Lett. **70**, 1895 (1993).

[7] C. H. Bennett and S. Wiesner, Phys. Rev. Lett. **69**, 2881 (1992).

[8] A. K. Ekert, Phys. Rev. Lett. **67**, 661 (1991).

[9] M. Hillery, V. Bužek, and A. Berthiaume, Phys. Rev. A **59**, 1829 (1999).

[10] A. V. Thapliyal, Phys. Rev. A **59**, 3336 (1999); J. Kempe, Phys. Rev. A **60**, 910 (1999); D. Dür and J. I. Cirac, e-print quant-ph/0011025.

[11] V. Coffman, J. Kundu, and W. K. Wootters, Phys. Rev. A **61**, 052306 (2000).

[12] W. K. Wootters, e-print quant-ph/0001114.

[13] W. Dür, e-print quant-ph/0006105.

[14] M. Koashi, V. Bužek, and N. Imoto, Phys. Rev. A **62**, 050302(R) (2000).

[15] S. Hill and W. K. Wootters, Phys. Rev. Lett. **78**, 5022 (1997); W. K. Wootters, *ibid.* **80**, 2245 (1998).

[16] J. I. Cirac and P. Zoller, Phys. Rev. Lett. **74**, 4091 (1995).

[17] A. Barenco, C. H. Bennett, R. Cleve, D. P. DiVincenzo, N. Margolus, P. W. Shor, T. Sleator, J. A. Smolin, and H. Weinfurter, Phys. Rev. A **52**, 3457 (1995).

[18] D. J. Wineland, C. Monroe, W. M. Itano, B. E. King, D. Leibfried, D. M. Meekhof, C. Myatt, and C. Wood, Fortschr. Phys. **46**, 363 (1998).

[19] F. Schmidt-Kaler, Ch. F. Roos, H. C. Nägerl, H. Rohde, S. Gulde, A. Mundt, M. Lederbauer, G. Thalhammer, Th. Zeiger, P. Barton, L. Hornekaer, G. Reymond, D. Leibfried, J. Eschner, and R. Blatt, J. Mod. Opt. **47**, 2573 (2000).

[20] A. Steane, Appl. Phys. B: Lasers Opt. **64**, 623 (1997) (see also e-print quant-ph/9608011).

[21] D. F. V. James, Appl. Phys. B: Lasers Opt. **66**, 181 (1998) (see also e-print quant-ph/9702053).

[22] A. Steane, C. F. Roos, D. Stevens, A. Mundt, D. Leibfried, F. Schmidt-Kaler, and R. Blatt, e-print quant-ph/0003087.

[23] H. C. Nägerl, Ch. F. Roos, H. Rohde, D. Leibfried, J. Eschner, F. Schmidt-Kaler, and R. Blatt, Fortschr. Phys. **48**, 623 (2000).